Principles of Adaptive Sorting Revealed by *In Silico* Evolution

Jean-Benoît Lalanne and Paul François
Physics Department, McGill University, Montreal, Quebec, Canada H3A 2T8
(Received 8 February 2013; published 21 May 2013)

Many biological networks have to filter out useful information from a vast excess of spurious interactions. In this Letter, we use computational evolution to predict design features of networks processing ligand categorization. The important problem of early immune response is considered as a case study. Rounds of evolution with different constraints uncover elaborations of the same network motif we name "adaptive sorting." Corresponding network substructures can be identified in current models of immune recognition. Our work draws a deep analogy between immune recognition and biochemical adaptation.

DOI: 10.1103/PhysRevLett.110.218102 PACS numbers: 87.16.Xa, 05.10.−a, 87.18.Mp, 87.18.Tt

Information processing in biology often relies on complex out-of-equilibrium physical processes ensuring efficiency [1]. The paradigmatic example is kinetic proofreading (KPR), first proposed to explain low spurious base-pair interactions during DNA replication [2,3]. KPR originated in a context with comparable concentrations of correct and spurious substrates. If the spurious substrate has similar characteristics and is orders of magnitude higher in concentration than the correct one, alternative strategies are needed.

An important instance of this problem is immune recognition by T cells. T cells constantly scan antigen presenting cells (APCs) in their environment, via the binding of their T cell receptors (TCRs) to the presented pMHC ligands. T cells perform a sorting process based on interaction with self (nonagonist) or foreign (agonist) ligands at the surface of APCs: if foreign ligands are detected, then the immune response is triggered. Following the "lifetime" dogma [4], one of the main determinants for distinguishing self from foreign is the unbinding time of the pMHC ligand to the TCR. Ligands up to a critical binding time of $\tau_c \simeq 3$ s do not elicit response while foreign ligands bound for a longer time ($\tau_f > \tau_c$) do. Self-ligands dissociate rapidly (typically for $\tau_s \lesssim 0.1$ s).

The sorting process is extremely sensitive: response is triggered in the presence of minute concentrations of foreign ligands ($\lesssim$10 ligands per cell [5,6]). Sorting is specific: although foreign (τ_f) and critical ligands (τ_c) have similar binding times, an arbitrary concentration of critical ligands does not elicit response [7]. These requirements are summarized in Fig. 1. McKeithan [8] proposed first that T cells harness the amplifying properties of KPR to solve the recognition problem between few foreign ligands and vastly numerous self-ligands. However, this model cannot account for sharp thresholding required for sensitivity and specificity [7]. Other control structures must exist.

In this Letter, we use computational evolution [9] to ask the related "inverse problem" question: How can a network categorize sharply two ligands with similar affinity irrespective of their concentrations? We discover and study analytically a new network module that we name "adaptive sorting." Extensive simulations show how it is improved to solve the related recognition problem of parallel sorting of foreign ligands within a sea of self-ligands. We expect the principles presented here to have broader relevance for biological recognition systems where specific signals must be extracted from a high number of weak spurious interactions.

Methods.—The algorithm we use to generate biochemical networks is essentially the same as in [10] with a biochemical grammar adapted to the problem of immune ligand recognition. Following [7], we limit possible interactions to phosphorylations or dephosphorylations with rates linear in enzyme concentrations. Ligands bind TCRs outside the cell, resulting in the activation of the internal part of the receptor [denoted by C_0, see Figs. 1(a) and 1(b)]. The algorithm then proceeds to add or remove kinases or phosphatases to evolve cascades of reactions downstream of C_0. We make the classical hypothesis underlying KPR models [8] that when a ligand dissociates

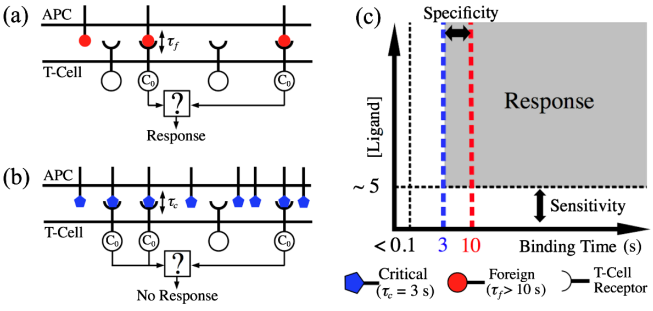

FIG. 1 (color online). Problem setup. (a) Few foreign ligand ($\tau_f > 10$ s) trigger response. (b) Arbitrary large concentrations of critical agonist ($\tau_c = 3$ s) ligands do not trigger response. (c) Idealization of the number of pMHC ligands required to trigger response as a function of pMHC-TCR binding time. Shaded region corresponds to conditions for which the immune response is triggered.

from a receptor, the receptor's internal part gets quickly dephosphorylated, an assumption consistent with the "kinetic segregation" mechanism [11] (see details in [12]). We assume that a single species in the network plays the role of the output of the system and triggers immune response in a binary way via a thresholding mechanism. The nature of the output is under selective pressure and can be changed by the algorithm.

The goal here is to discriminate between two kinds of ligands with identical on-rate (denoted by κ) but different binding times (foreign: $\tau_f = 10$ s, critical: $\tau_c = 3$ s; we checked that the results presented are independent of specific τs as long as τ_f/τ_c is not too big). For pure KPR [8], the concentration of the output is linear in ligand concentration. Thus, as shown in Fig. 2(a), ligands with similar binding times are distinguished by a thresholding mechanism only over a limited range of concentration, even for a large number of proofreading steps [7]. In contrast, if the steady state output concentration is almost flat in ligand concentration due to some control mechanism, e.g., in Fig. 2(b), then ligands can be categorized by thresholding nearly irrespective of their concentration.

To select for networks producing almost flat ligand dependency, we sample logarithmically the range of allowed ligand concentration. Steady state outputs are computed for sampled ligand concentrations and binned for the two binding times considered [Fig. 2(c) shows the binned outputs corresponding to Fig. 2(b)]. We then consider the histograms of output for different τ's as an effective probability

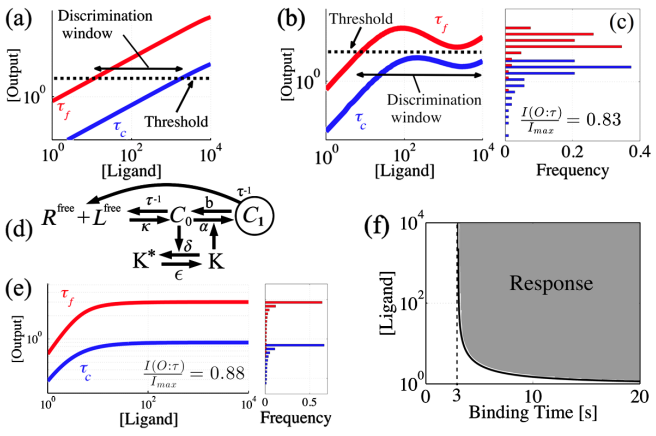

FIG. 2 (color online). (a) The KPR scheme has discrimination abilities over a limited range of ligand concentration. (b) Output vs ligand for $\tau_f = 10$ s and $\tau_c = 3$ s. (c) Histogram of outputs from (b) illustrating effective probability distribution. (d) Adaptive sorting network. Arrows with no specified enzyme represent unregulated reactions. The output is circled. We keep conventions throughout. (e) Output vs ligand and histogram of output for adaptive sorting ($\kappa = 10^{-4}$, $R = 10^4$, $\delta = 1$, $\epsilon = 1$, $\alpha = 3 \times 10^{-4}$, $b = 0$, and $K_T = 10^3$). (f) Minimum ligand concentration triggering response for different binding times for adaptive sorting in (e). Threshold taken to be $\xi(\tau_c)$.

distribution function. A natural measure of performance ("fitness") selecting for networks with behavior similar to Fig. 2(b) is then the mutual information, $\mathcal{I}(O; \tau = \{\tau_c, \tau_f\})$ [13], between the output value and the dissociation time. A network for which $\mathcal{I}(O;\tau) = \mathcal{I}_{\max}(= 1$ bit) has its output distributions for τ_f and τ_c disjoint, corresponding to a perfect discrimination. We take this as our fitness function. More details on the evolutionary simulations are given in [12].

Simple adaptive sorting.—We run our simulations with deterministic integration of network equations. Figure 2(d) presents a typical network topology we obtain, with the corresponding distribution of outputs on Fig. 2(e). Distributions corresponding to the two binding times are clearly separated. In this network, C_0 is phosphorylated to C_1 by kinase K. K is itself phosphorylated by C_0, making it inactive. C_1 is the output. Calling R, L, and K_T the total concentration of receptors, ligands, and kinase, respectively, equations for this network are

$$\dot{C}_0 = \kappa R^{\text{free}} L^{\text{free}} - (\alpha K + \tau^{-1}) C_0 + b C_1, \tag{1}$$

$$\dot{C}_1 = \alpha K C_0 - (\tau^{-1} + b) C_1, \tag{2}$$

$$\dot{K} = -\delta C_0 K + \epsilon (K_T - K). \tag{3}$$

$R^{\text{free}} = R - \sum_{i=0}^{1} C_i$ and $L^{\text{free}} = L - \sum_{i=0}^{1} C_i$ are the concentrations of free receptors and ligands. Assuming receptors are in excess ($R^{\text{free}} \simeq R$), the steady state concentration of output variable C_1 can be computed. We get $C_1 = \xi(\tau) C_0/(C_0 + C_*)$ where $\xi(\tau) = \alpha K_T C_*/(b + \tau^{-1})$, $C_* = \epsilon \delta^{-1}$.

For large L, $C_0 \propto L$. In particular, as $C_0 \gg C_*$, $C_1 \simeq \xi(\tau)$. It is also clear that even for small L, C_1 will be a pure function of τ independent from L if C_* is small enough. To discriminate between two ligands with binding times τ_1 and τ_2, one then simply needs to assume response is activated for a C_1 threshold value $\theta \in [\xi(\tau_1), \xi(\tau_2)]$. Figure 2(f) illustrates the range in ligand concentration leading to a response with such a thresholding process for the present network. The network shows both extremely good sensitivity and specificity [cf. Fig. 1(c)].

This situation is reminiscent of biochemical adaptation, where one variable returns to the same steady state value irrespective of ligand concentration. Indeed, the motif displayed on Fig. 2(c) implements an "incoherent feedforward loop" as observed in adaptive systems [10,14,15]: C_0 feeds negatively into kinase K, and both C_0 and K feed positively into output C_1. The overall influence of C_0 (and of L) is a balance between two opposite effects which cancel out. One significant difference from classical adaptation is that the steady state concentration of C_1 is now a function of the extra parameter τ, the ligand dissociation time. Discrimination of ligands based on the value of the output becomes possible irrespective of the ligand concentrations.

This process can be generalized to other adaptive networks based on ligand-receptor interactions, as long as one kinetic parameter is ligand specific. For instance, ligand-receptor networks evolved in [10] can be modified to have a steady state concentration depending on ligand nature. Call I the input, R the receptor, and C the resulting complex. The adaptive system $\dot{R} = \rho - IR$ and $\dot{C} = IR - C/\tau_I$ stabilizes to a steady state concentration $C = \rho\tau_I$, which depends only on τ_I irrespective of input value. Such combination of biochemical adaptation with a kinetic parameter dependency could potentially be observed in a wide variety of biochemical networks. We call it *adaptive sorting*.

Parallel adaptive sorting.—Adaptive sorting by itself is efficient to discriminate independently critical from foreign ligands, but its performance is degraded when cells are exposed *at the same time* to foreign ligands (concentration L_f) and a huge excess of self-ligands (concentration L_s), as illustrated in Fig. 3(a). This phenomenon is called antagonism [7]. Performance is degraded because the two different kinds of ligands are coupled through the common kinase used in the feedforward motif [dashed arrows in Fig. 3(b)]. Precisely, denoting the complexes arising from the binding of foreign and self-ligands by C_i and D_i respectively, the total output concentration is

$$C_1 + D_1 \simeq C_1 = \frac{\xi(\tau_f) C_0}{C_0 + D_0 + C_*}, \tag{4}$$

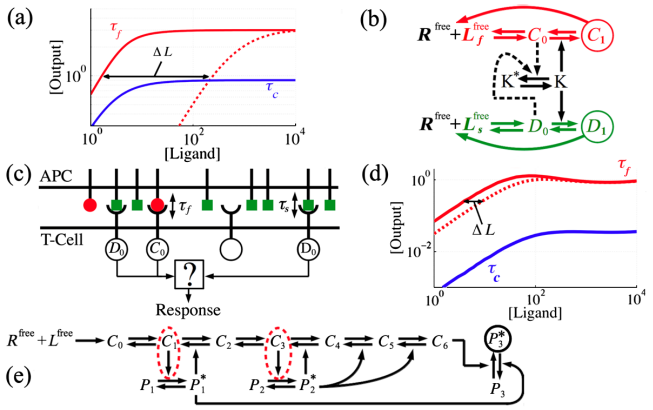

FIG. 3 (color online). (a) Effect of self-ligands on the adaptive sorting module from Fig. 2(e), taking $[C_N] + [D_N]$ as an output. Full lines: $L_s = 0$. Dashed line: $L_s = 10^4$. ΔL quantifies negative effect of self-ligands on sensitivity. We compare τ_f with $L_s > 0$ to τ_c with $L_s = 0$ as a worst case scenario. (b) Coupling (dashed arrows) between two different types of ligands through kinase K for adaptive sorting. (c) Schematic illustration of new constraint of parallel sorting. Squares represent self-ligands ($\tau_s = 0.05$ s). (d) Example of evolved output vs ligand relationship with $L_s = 0$ (full lines) and $L_s = 10^5$ (dashed line). Loss in sensitivity is now small. (e) Schematic of network corresponding to (d). Complexes C_i's are understood to decay to R^{free} and L^{free} (same convention in Fig. 4). Parameters are given in [12].

which still tends to $\xi(\tau_f)$ at large L_f. We can neglect D_1 in the output because $\xi(\tau) \propto \tau$ and so $\xi(\tau_s) \ll \xi(\tau_f)$. To reach the adaptive regime, we now have the requirement that $C_0 \gg D_0$. For large L_s, $D_0 \gg D_1$ and we have that $D_0 \approx D_0 + D_1 = \kappa R \tau_s (1 + \kappa R \tau_s)^{-1} L_s$. Similarly, $C_0 \simeq \kappa R \tau_f (1 + \kappa R \tau_f)^{-1} L_f$. Thus $C_1 \simeq \xi(\tau_f)$ for

$$L_f \gg \left(\frac{1 + \kappa R \tau_f}{1 + \kappa R \tau_s}\right)\left(\frac{\tau_s}{\tau_f}\right) L_s \sim \kappa R \tau_s L_s. \tag{5}$$

With $\kappa R \tau_f \gg 1$, $L_s \sim 10^5$, and $\kappa R \tau_s \sim 0.1$, self-ligands annihilate the simple adaptive sorting motif's sensitivity.

To solve this problem, we rerun evolutionary simulations with the constraint that discrimination between τ_f and τ_c should happen even in the massive presence of self-ligands ($\tau_s = 0.05$ s), as sketched in Fig. 3(c). A representative result of this computational evolution is presented in Figs. 3(d) and 3(e) for output and network topology, respectively. The networks found look very similar to adaptive sorting, except that the incoherent feedforward module is sometimes implemented via activation of a phosphatase, instead of deactivation of a kinase [16]. A full cascade of KPR also evolves. Notably, in all working networks there is an important difference with the previous case: activation of the enzyme in the adaptive sorting module is rewired downstream in the first step of the KPR cascade [dashed circles in Fig. 3(e)].

This can be understood analytically by considering an idealized network such as the one in Fig. 4(a) which is compared to the actual network implicated in immune response [7,17] in Fig. 4(b). Our idealization consists in an adaptive sorting module with upstream and downstream steps of KPR [N steps in total, adaptive module activated by complex m, $m + 2 \leq N$, Fig. 4(a)]. In such networks, assuming no dephosphorylation down the cascade ($b = 0$), the output takes the form [12]

$$C_N + D_N \simeq C_N = \frac{\xi'(\tau_f) C_0}{C_m + D_m + C_*(1 + \alpha K_T \tau_f)}, \tag{6}$$

where $C_m = \gamma_f^m C_0$ and $D_m = \gamma_s^m D_0$, with $\gamma_i = \phi\tau_i(1 + \phi\tau_i)^{-1}$. ϕ denotes the unregulated phosphorylation rate in the cascade. $\xi'(\tau)$ is a function of τ, and like before $\xi'(\tau_s) \ll \xi'(\tau_f)$ so that we can neglect the contribution of D_N in the output. Even in the presence of many self-ligands L_s, we have an output independent of L_f for $C_0 \gg \gamma_f^{-m}\gamma_s^m D_0$ ($m = 0$ is simple adaptive sorting). Since $\phi \sim \tau_f^{-1}$ for a sensitive network [12], $\gamma_s\gamma_f^{-1}$ is small; thus, any $m > 1$ makes $\gamma_f^{-m}\gamma_s^m$ even smaller. So this upstream proofreading cascade ensures that $C_m \gg D_m$ and the adaptive sorting module is only triggered by foreign ligands. As for simple adaptive sorting, we have that $C_0 \propto L_f$ and $D_0 \propto L_s$ although the prefactors differ [12]. In the end, C_N is a pure function of τ_f for

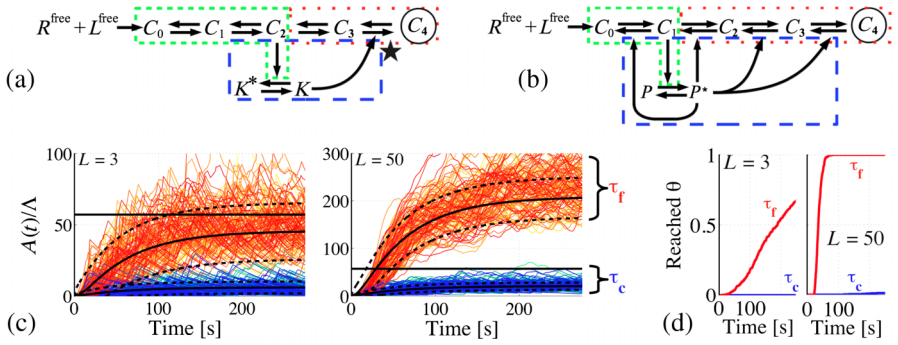

FIG. 4 (color online). (a) Final network with categorization properties in the presence of large concentrations of spurious substrates. The parallel (fine dash), adaptive (long dash) and KPR (dotted) modules are identified. Star indicates the specific phosphorylation in adaptive sorting. (b) Network for immune recognition with corresponding features, from Refs. [7,17]. (c) Sample trajectories of A for two ligand concentrations L. Horizontal line: threshold θ. Black curves are analytic expressions from [12]. (d) Fraction of trajectories having reached threshold. $N = 4$, $m = 2$, $\epsilon = 0.5$, $\phi = 0.3$, no self, other parameters as in Fig. 2.

$$L_f \gg \left(\frac{1 + \kappa R \tau_f}{1 + \kappa R \tau_s}\right)\left(\frac{\gamma_s}{\gamma_f}\right)^{m+1} L_s \qquad (7)$$

so that the right-hand side is small compared to Eq. (5) for $m > 0$. Self-influence is consequently almost abolished.

It must be emphasized that the solutions displayed in Figs. 3(e) and 4(a) require more than one kinase or phosphatase: generic enzymes are shared by most of the proofreading steps, while a specific enzyme accounts for the adaptive sorting module [star in Fig. 4(a)]. This is of biological importance since it is not clear that biochemistry would allow fine-tuned specificity to a single step in the cascade. Interestingly, alternative solutions also evolve where kinases and phosphatases are not specific to a given proofreading step [12]. For these networks, discrimination is still possible, but loss of biochemical specificity degrades the adaptive properties. One observes a nonmonotonic behavior, approximately flattened out over the range of input ligand considered, as seen in [17].

Dealing with low numbers of molecules.—Immune cells perform efficient sorting of different ligand types for as little as $\sim$10 foreign ligands. A low number of molecules is potentially problematic because adaptive sorting shows a trade-off between specificity and sensitivity. In the simpler scheme [Fig. 2(c)], perfect adaptation occurs for all L if $C_* \to 0$, but the adaptive output value is $C_1 = \xi(\tau) \propto C_* \to 0$ so that discrimination becomes impossible. Increasing N actually softens the constraint: downstream KPR steps [Fig. 4(a)] add a geometric dependency in τ to C_N (specificity) even for low C_* (sensitivity) [12].

A related problem is fluctuations at low ligand numbers. In the immune context, phosphorylated tails of receptors (corresponding to C_N) slowly phosphorylate abundant ($> 10^4$) downstream targets. Following [17], we pose a variable A (slow downstream species) obeying $\dot{A} = \Lambda C_N - T^{-1}A$. For $T \gg \tau$, A effectively time averages the output C_N, thereby smoothing out fluctuations. A can realistically be assumed deterministic as long as Λ is large: the only A stochasticity comes from C_N. We assume thresholding is then made on A, leading to a binary *irreversible* decision [18]. We take $T = 60$ s, as response occurs on the order of minutes [7].

Simulations of this process using the Gillespie algorithm [19] are presented in Figs. 4(c) and 4(d), with samples of trajectories and the fraction of activated cells as a function of time. Results are in very good agreement with a simple linear noise approximation on C_N (see details and assumptions in [12]). Ligands at τ_c essentially never cross the threshold for the considered time window, while for ligands at τ_f, almost all cells eventually respond for $L_f \lesssim 10$. Finally, the model's half population response time [Fig. 4(d)] is consistent with experiments [7,12,17] and decreases down to less than one minute as L_f increases. So, although we cannot exclude that other noise-resistance mechanisms are possible [20], adaptive sorting coupled to a slow downstream cascade has discrimination capabilities compatible with experimental data.

Our final model is summarized in Fig. 4(a) and shares many similarities with network features of the immune system Fig. 4(b) [17]. In our framework, immune recognition corresponds to an optimal solution with nonspecific enzymes. Adaptive sorting manifests itself through nonlinear dependency of response on input concentration, which is observed in a wide range of signalling networks (e.g., endocrine signalling [21]), and could lie at the core of such signalling processes as well as others.

We thank Eric Siggia, Massimo Vergassola, Guillaume Voisinne, and Grégoire Altan-Bonnet for useful discussions. J.-B. L. is supported by the Natural Sciences and Engineering Research Council of Canada (NSERC), P. F. by NSERC and the Human Frontier Science Program.

[1] P. S. Swain and E. D. Siggia, Biophys. J. **82**, 2928 (2002).
[2] J. J. Hopfield, Proc. Natl. Acad. Sci. U.S.A. **71**, 4135 (1974).
[3] J. Ninio, Biochimie **57**, 587 (1975).

[4] O. Feinerman, R. N. Germain, and G. Altan-Bonnet, Molecular immunology **45**, 619 (2008).
[5] D. J. Irvine, M. A. Purbhoo, M. Krogsgaard, and M. M. Davis, Nature (London) **419**, 845 (2002).
[6] O. Feinerman, J. Veiga, J. R. Dorfman, R. N. Germain, and G. Altan-Bonnet, Science **321**, 1081 (2008).
[7] G. Altan-Bonnet and R. N. Germain, PLoS Biol. **3**, e356 (2005).
[8] T. W. Mckeithan, Proc. Natl. Acad. Sci. U.S.A. **92**, 5042 (1995).
[9] P. François and V. Hakim, Proc. Natl. Acad. Sci. U.S.A. **101**, 580 (2004).
[10] P. François and E. D. Siggia, Phys. Biol. **5**, 026009 (2008).
[11] S. J. Davis and P. A. van der Merwe, Nat. Immunol. **7**, 803 (2006).
[12] See Supplemental Material at http://link.aps.org/supplemental/10.1103/PhysRevLett.110.218102 for detailed derivation of equations, discussion of assumptions, and additional examples of results of *in silico* evolution.
[13] G. Tkačik and A. M. Walczak, J. Phys. Condens. Matter **23**, 153102 (2011).
[14] M. Behar, N. Hao, H. G. Dohlman, and T. C. Elston, Biophys. J. **93**, 806 (2007).
[15] W. Ma, A. Trusina, H. El-Samad, W. A. Lim, and C. Tang, Cell **138**, 760 (2009).
[16] It can be shown that regulation via the phosphatase indeed requires at least two phosphorylation steps, explaining why it is less probable to evolve compared to the motif of Fig. 2(d) when no other constraint is imposed.
[17] P. François, G. Voisinne, E. D. Siggia, G. Altan-Bonnet, and M. Vergassola, Proc. Natl. Acad. Sci. U.S.A. **110**, E888 (2013).
[18] T. Lipniacki, B. Hat, J. R. Faeder, and W. S. Hlavacek, J. Theor. Biol. **254**, 110 (2008).
[19] D. T. Gillespie, J. Phys. Chem. **81**, 2340 (1977).
[20] D. C. Wylie, J. Das, and A. K. Chakraborty, Proc. Natl. Acad. Sci. U.S.A. **104**, 5533 (2007).
[21] L. N. Vandenberg, T. Colborn, T. B. Hayes, J. J. Heindel, D. R. Jacobs, D. H. Lee, T. Shioda, A. M. Soto, F. S. vom Saal, W. V. Welshons, R. T. Zoeller, and J. P. Myers, Endocrine reviews **33**, 378 (2012).